In-wheel vehicle control implementation with energy and safety considerations

A. Mihály and P. Gáspár and B. Németh

Abstract The paper deals with the energy optimal and reconfigurable control of a four-wheel independently-actuated (4WIA) vehicle operated by in-wheel hub motors and a steer-by-wire steering system mounted on the front axle. In the proposed setup the vehicle maneuvers around corners by using the powerful torque vectoring capability of the electric in-wheel motors, while steering is only applied when a fault event of a hub motor is detected or the cornering resistance of the vehicle can be reduced by it. The steering intervention is realized by a high-level control reconfiguration based on the LPV (Linear Parameter Varying) method. The operation of the introduced method is tested in CarSim simulation environment.

1 Introduction

As economical and environment friendly hybrid/electric vehicles become more and more popular, researchers and automotive companies also focus on the development of in-wheel electric vehicles. One of the main constructional benefits of in-wheel vehicles is the space-efficient passenger cabin design, which is essential for small city cars. From a vehicle dynamic point of view the independent, fast and precise torque generation of the hub motors lends torque vectoring capability to the vehicle with which maneuverability can be enhanced significantly, see [16, 9, 17, 2]. By knowing the characteristics of the in-wheel engines and the hydraulic brake system,

A. Mihály
Institute for Computer Science and Control Hungarian Academy of Sciences and MTA-BME Control Engineering Research Group, Budapest, Hungary, e-mail: mihaly.andras@sztaki.mta.hu

P. Gáspár and B. Németh
Institute for Computer Science and Control Hungarian Academy of Sciences, Budapest, Hungary
e-mail: [peter.gaspar;balazs.nemeth]@sztaki.mta.hu

energy optimal torque distribution and high efficiency regenerative braking can be implemented, as proposed by [3, 13, 12, 8]

This paper focuses on the trajectory and velocity tracking of a 4WIA vehicle equipped with four in-wheel electric motors and a steer-by-wire steering system. The aim of the design is to establish a control architecture capable of satisfying multiple requirements related to energy efficiency and safety, using high level control reconfiguration between steering and yaw-moment generation.

The paper is organized as follows: Section 2 introduces the control reconfiguration scheme used for the trajectory tracking of the 4WIA vehicle with safety and efficiency considerations. Section 3 deals with the implementation of the proposed control architecture in a hierarchical structure. Section 4 demonstrates the effect of the introduced method in CarSim simulation environment. Finally, some conclusive statements are listed in Section 5.

2 Design of control signals

The goal of the design is to ensure trajectory and velocity tracking for the 4WIA vehicle taking longitudinal and lateral dynamics into account. Thus, for the modeling of the 4WIA vehicle dynamics, the well known two-wheeled bicycle model is used, see Figure 1. The motion equations in the planar plane can be written as follows:

$$J\ddot{\psi} = c_1 l_1 \alpha_1 - c_2 l_2 \alpha_2 + M_z \tag{1a}$$

$$m\dot{\xi}(\dot{\psi} + \dot{\beta}) = c_1 \alpha_1 + c_2 \alpha_2 \tag{1b}$$

$$m\ddot{\xi} = F_l - F_d \tag{1c}$$

where the vehicle mass is noted with m, the yaw inertia with J, the tyres lateral stiffness with c_1 and c_2 for the front and rear wheels. The distances measured from the center of gravity to the front and rear axes are represented with l_1 and l_2. The side slip angles of the front and rear wheels are $\alpha_1 = \delta - \beta - \dot{\psi} l_1/\dot{\xi}$ and $\alpha_2 = -\beta + \dot{\psi} l_2/\dot{\xi}$. The yaw rate of the vehicle is indicated by $\dot{\psi}$, the vehicle side-slip angle is β and ξ is the longitudinal displacement of the 4WIA vehicle.

The high-level control inputs of the vehicle are the longitudinal force noted with F_l, the yaw moment M_z generated by torque vectoring, and the steering angle δ of the front wheels. In the design of the proposed trajectory and velocity tracking controller, longitudinal disturbance forces originating from the drag, the slope of the road and the wheel rolling resistance is also considered as:

$$F_d = 0.5 C_d \rho A_F \dot{\xi}^2 + mg \sin \alpha_s + mgf \cos \alpha_s,$$

where C_d is the aerodynamic drag coefficient, ρ is the air density, A_F is the contact surface of the vehicle, α_s describes the road inclination angle, f is the road friction coefficient connected to rolling resistance, while g is the gravitational constant.

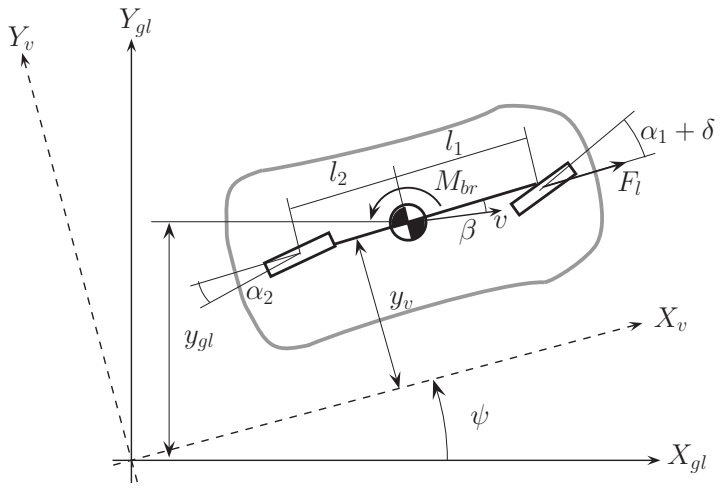

Fig. 1 Single track bicycle model

Since the nonlinearity of the system described by the differential equations of (1) is caused by the velocity $\dot{\xi}$ of the vehicle, choosing it as a scheduling variable $\rho_1 = \dot{\xi}$ the nonlinear model is rewritten as an LPV model.

For the nonlinear model of the 4WIA vehicle a gain scheduling LPV controller is necessary to guarantee a global solution, see [1, 6]. The reference signals for the vehicle to follow are the reference velocity and the yaw rate. The former is set by the driver, while the latter is also given by the driver steering intervention δ_d as follows [7]: $\dot{\psi}_{ref} = v/d \cdot e^{-\frac{t}{\tau}} \cdot \delta_d$, where τ is the time constant, d is a parameter depending on the vehicle geometry and velocity.

The *LPV* control synthesis detailed in [15] is realized such way that energy efficiency and safety can be considered with modifying the value of the scheduling variable ρ_2 responsible for the allocation between the steering δ and the yaw moment generation M_z. In this paper, the fault tolerant reconfiguration process detailed in [4] is enhanced by energy consumption consideration. The aim of the cornering resistance minimization technique is to find a balance between steering angle δ and yaw moment M_z in such a way, that the energy consumption related to the cornering effort is minimized. Thus, the value of ρ_2 responsible for the scaling of the actuators is defined based on a calculation introduced in [5]. Note, that in case of a fault event or skidding this value of ρ_2 is overwritten with that given by the safety calculation introduced in [4].

3 Implementation of the proposed control system

The trajectory and velocity tracking control system of the 4WIA vehicle augmented with fault tolerant and energy optimal reconfiguration is implemented in a multi-layer, hierarchical structure, as shown in Figure 2.

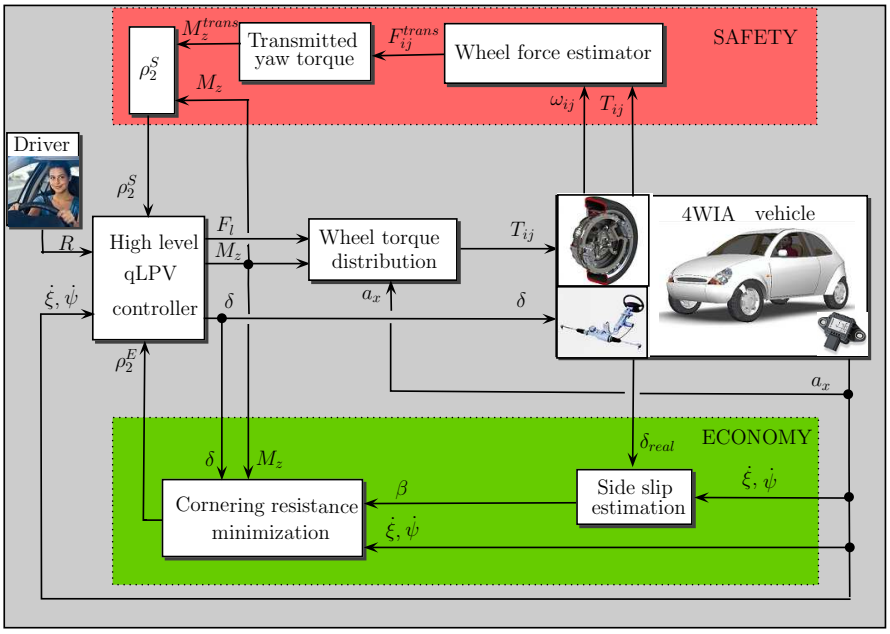

Fig. 2 Scheme of the 4WIA reconfigurable control

The first layer consists of the high-level LPV controller, calculating the inputs of the 4WIA vehicle based on the reference signals provided by the driver, the measured vehicle signals (velocity and yaw rate) and the current value of the scheduling variable ρ_2. The latter is defined based on the calculated values detailed in Section 2, using a simple decision logic. Giving higher priority to vehicle safety than energy optimality, the value of ρ_2 is specified as follows:

$$\rho_2 = \begin{cases} \rho_2^E, & \text{if } \rho_2^E > \rho_2^S \\ \rho_2^S, & \text{if } \rho_2^E \leq \rho_2^S \end{cases} \tag{2}$$

Since chattering between controllers must be avoided, a first-order proportional filter and a hysteresis component are applied to ρ_2.

The function of the second layer is to allocate the signals given by the high-level controller between the actuators of the 4WIA vehicle. Here a dynamic allocation method considering pitch dynamic is used, already presented in [4], thus here only the results are presented. The longitudinal wheel forces determined by the input

signals of the high-level controller are the following:

$$F_{fL} = \frac{F_l}{2\left(1+\frac{1}{\kappa}\right)} - \frac{M_z}{b_f + \frac{1}{\kappa} b_r}, \quad F_{rL} = \left(\frac{1}{\kappa}\right) F_{fL},$$
$$F_{fR} = \frac{F_l}{2\left(1+\frac{1}{\kappa}\right)} + \frac{M_z}{b_f + \frac{1}{\kappa} b_r}, \quad F_{rR} = \left(\frac{1}{\kappa}\right) F_{fR} \tag{3}$$

where F_{ij} $i \in [f = front, r = rear]$, $j \in [L = left, R = right]$ are the wheel forces, b_f and b_r are the front and rear track, κ stands for the load distribution between the front and rear axle which can be determined measuring the longitudinal acceleration of the vehicle with an accelerometer. Thus, the wheel torques needed to be produced by the in-wheel hub motors are given as $T_{ij} = R_{eff} F_{ij}$, where R_{eff} is the effective rolling radius of the tyres.

The third layer consists of the low-level controllers connected to the steer-by-wire steering system and the in-wheel electric motors. The aim of the last layer it to transform the allocated control signals into real physical parameters of the actuators. Here, the steering system is considered to be a simple first order system as proposed by [11], while the torque generation of the in-wheel engines are regarded as a second-order system (see [10]) with the following transfer function:

$$T_{motor}(s) = \frac{T(s)(1+\eta)}{1+2\zeta+2\zeta^2} \tag{4}$$

where T is the desired torque given by the second layer of the hierarchical control system, T_{motor} is the real output torque, while ζ and η are parameters related to the response time and steady state error of the in-wheel motor.

The measured signals of the vehicle used for the calculation of ρ_2^S are the in-wheel motor torques T_{ij}, the angular acceleration of the wheels $\dot{\omega}_{ij}$ assumed to be measured by wheel sensors. The strategy is based on the assumption that, given the in-wheel motors fast and accurate torque generation, the transmitted torque can be estimated precisely with the motion equation of the wheels, written as follows:

$$J_\omega \dot{\omega}_{ij} = T_{ij} - R_{eff} F_{ij}, \tag{5}$$

where J_ω is the wheel inertia, T_{ij} is the torque produced by the wheel hub motor. Hence, drive force F_{ij} and the related transmitted yaw torque can be estimated. By this mean, the value of ρ_2^S can be calculated for the high level LPV controller.

The vehicle lateral acceleration is measured by accelerometer on order to evaluate the wheel torque allocation of the second layer. The velocity of the vehicle is given by the wheel speeds, while yaw rate can be measured by gyro sensors. These measurement data are used in the high level LPV controller of the first layer as well as the cornering resistance calculation. Note, that the vehicle side slip angle is approximated with rearranging the equation given by [7] as:

$$\beta = arccos\left(\frac{\dot{\psi}(l_1+l_2)}{\dot{\xi}tan(\delta)}\right) \tag{6}$$

Hence, by knowing the actual steering angle and generated yaw moment the value of ρ_2^E can be defined for the high level controller, see [5].

4 Simulation results

Simulation has been performed in CarSim with a small 4WIA vehicle equipped with four in-wheel motors and a steer-by-wire steering system. The physical parameters of the electric hub motors based on specifications given by [14] are shown in Table 1.

Table 1 Electric motor specifications

Parameter	Value	Unit
Total motor mass	34	kg
Peak output power	75	kW
Continuous output power	54	kW
Peak output torque	1000	Nm
Continuous output torque	650	Nm
Nominal input voltage range	$200-400$	Vdc

Other physical parameters of the 4WIA vehicle including mass, aerodynamic coefficient, suspension geometry and wheel cornering stiffness are those of a conventional A-Class vehicle, see Table 2.

Table 2 Parameters of the 4WIA vehicle

Parameter	Value	Unit
Vehicle mass (m)	830	kg
Yaw moment of inertia (J)	1110.9	kgm^2
Distance from C.G to front axle (l_1)	1.103	m
Distance from C.G to rear axle (l_2)	1.244	m
Tread front (b_f)	1.416	m
Tread rear (b_r)	1.375	m
Height of COG (h_{COG})	0.54	m
Cornering stiffness front (c_1)	22	kN/rad
Cornering stiffness rear (c_2)	85	kN/rad
Aerodynamic drag co-efficient (c_w)	0.343	$-$
Front contact surface (A)	1.6	m^2

In the simulation the 4WIA vehicle driven by a driver must follow the trajectory of an S-turn, see Figure 3(a). The velocity of the vehicle is set at a constant target speed of 40 km/h as shown in Figure 3(b), while the yaw rate for the vehicle to follow given by the road curvature and vehicle velocity is demonstrated in Figure 3(c).

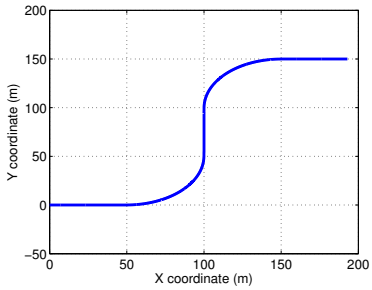

(a) Geometry of the S-turn

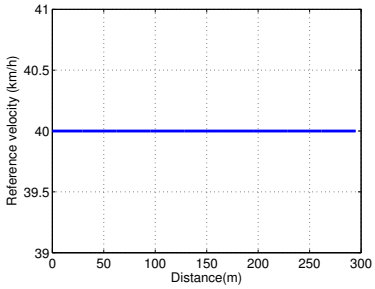

(b) Reference velocity

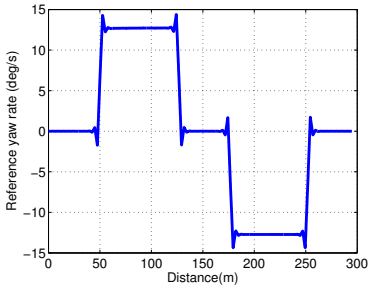

(c) Reference yaw rate

Fig. 3 Reference signals

During the simulation it is assumed that certain dynamic parameters of the 4WIA vehicle including yaw rate, planar plane accelerations and wheel speeds can be measured in order to assess the proposed reconfiguration strategy as well as the wheel force distribution.

The purpose of the simulation is to reveal the advantages of the energy optimal high-level control distribution, as the fault tolerant properties of the design have already been demonstrated in [4]. Hence, in the present simulation it is assumed that actuators in the in-wheel vehicle operate adequately without any fault event.

Two simulations have been evaluated with different vehicle set-up in order to study the effect of the proposed method. In the first case the 4WIA vehicle is operated relying entirely on the torque generation of its in-wheel motors, thus no steering is applied. The second simulation demonstrates the effect of the proposed reconfiguration method focusing on the cornering resistance minimization technique.

The high-level control signals depicted in Figure 4 are different for the two cases as a result of the selection of ρ_2. Although the longitudinal control signals are similar in both cases (see Figure 4(a)), only the vehicle applying the proposed method operates the steering system during cornering, as shown in Figure 4(b). Note that at the same time the yaw moment is reduced significantly (see Figure 4(c)).

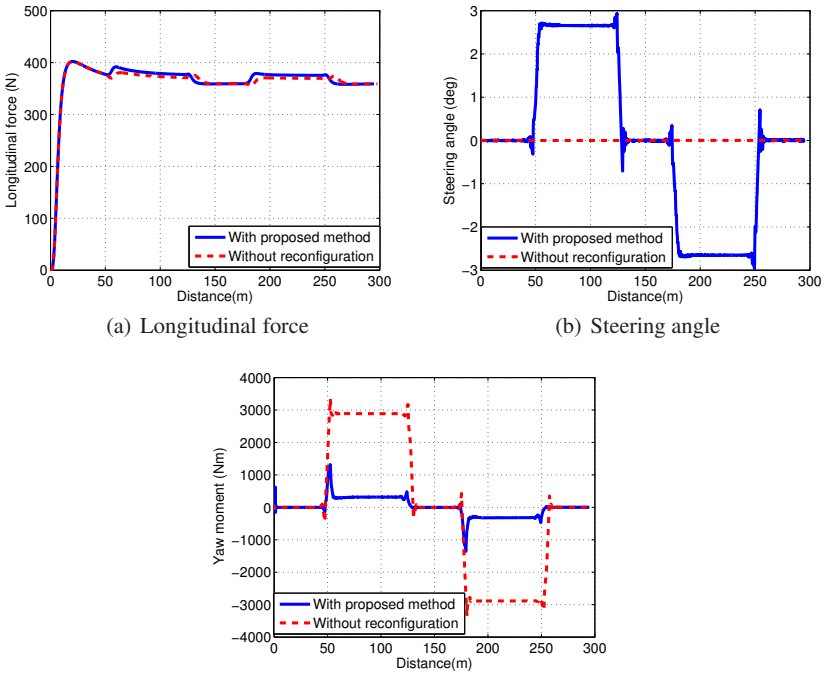

(a) Longitudinal force

(b) Steering angle

(c) Yaw moment

Fig. 4 High-level control signals

In Figure 5 the torque generations of the in-wheel motors are shown for the two cases. The 4WIA vehicle utilizing only its torque vectoring ability generates much greater amount of differential torque, as it can be observed in Figure 5(a). In contrast, with the proposed method the generated differential torques are smaller, hence the in-wheel motor torques are moderated as well.

Next, the control performances are shown in Figure 6 for the two different cases. It can be observed that the velocity error (see Figure 6(a)) and yaw rate error (see Figure 6(b)) are very similar for both cases, with a slightly better reference yaw rate following performance achieved with the proposed method. The energy loss due to cornering resistance shown in Figure 6(c) clearly demonstrated the advantage of the proposed method. As it can be observed a significant amount of energy can be saved with the energy optimal control allocation, which contributes to the approximately 10% of reduction in total energy consumption, see Figure 6(d).

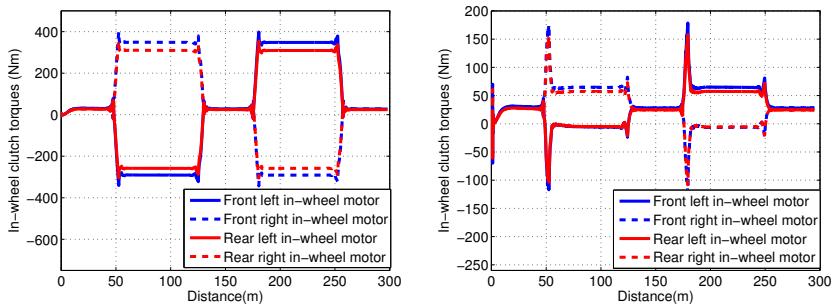

(a) Without proposed method (b) With proposed method

Fig. 5 Hub motor torques

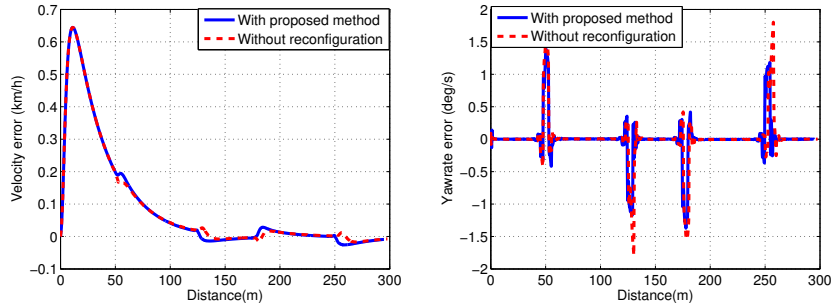

(a) Velocity error (b) Yawrate error

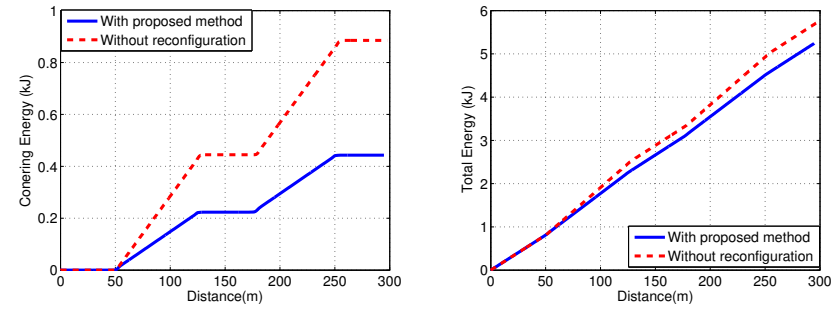

(c) Cornering energy (d) Total energy

Fig. 6 Performances of different methods

5 Conclusion

The paper has presented a velocity and trajectory tracking reconfiguration control method for 4WIA in-wheel vehicles with a steer-by-wire steering system. The aim

of the proposed method is to create both an energy optimal and fault tolerant control allocation between the vehicle actuators during cornering. By this means the efficiency of the in-wheel vehicle can be increased, while the safety of the vehicle can be guaranteed in case of a fault event or skidding. The operation of the proposed reconfiguration method has been demonstrated in CarSim simulation environment.

Acknowledgements The research was supported by the National Research, Development and Innovation Fund through the project "SEPPAC: Safety and Economic Platform for Partially Automated Commercial vehicles" (VKSZ 14-1-2015-0125).

References

[1] J. Bokor and G. Balas. Linear parameter varying systems: A geometric theory and applications. *16th IFAC World Congress, Prague*, 2005.

[2] R. Castro, R. E. Araújo, M. Tanelli, S. M. Savaresi, and D. Freitas. Torque blending and wheel slip control in evs with in-wheel motors. *Vehicle System Dynamics*, 50:71–94, 2012.

[3] C. Lin Cheng and Z. Xu. Wheel torque distribution of four-wheel-drive electric vehicles based on multi-objective optimization. *Energies 2015*, 8:3815–3831, 2015.

[4] P. Gáspár, J. Bokor, A. Mihály, Z. Szabó, T. Fülep, and F. Szauter. Robust reconfigurable control for in-wheel electric vehicles. *9th IFAC Symposium on Fault Detection, Supervision and Safety for Technical Processes (SAFEPROCESS'15)*, pages 36–41, 2015.

[5] A. Mihály and P. Gáspár. Robust and fault-tolerant control of in-wheel vehicles with cornering resistance minimization. *European Control Conference (ECC'16)*, 2016. ACCEPTED.

[6] A. Packard and G. Balas. Theory and application of linear parameter varying control techniques. *American Control Conference, Workshop I, Albuquerque, New Mexico*, 1997.

[7] R. Rajamani. Vehicle dynamics and control. *Springer*, 2005.

[8] M. Ringdorfer and M. Horn. Development of a wheel slip actuator controller for electric vehicles using energy recuperation and hydraulic brake control. *IEEE International Conference on Control Applications, Denver, USA*, pages 313–318, 2011.

[9] Z. Shuai, H. Zhang, J. Wang, J. Li, and M. Ouyang. Lateral motion control for four-wheel-independent-drive electric vehicles using optimal torque allocation and dynamic message priority scheduling. *Control Engineering Practice*, 24:55–66, 2013.

[10] F. Tahami, R. Kazemi, and S. Farhanghi. A novel driver assist stability system for all-wheel-drive electric vehicles. *IEEE Transactions on Vehicular Technology*, 52:683–692, 2003.

[11] F. Takanori, M. Shogo, M. Kenji, A. Norihiko, and O. Koichi. Active steering systems based on model reference adaptive nonlinear control. *Vehicle System Dynamics: International Journal of Vehicle Mechanics and Mobility*, 42:301–318, 2004.

[12] B. Wang, X. Huang, J. Wang, X. Guo, and X. Zhu. A robust wheel slip ratio control design combining hydraulic and regenerative braking systems for in-wheel-motors-driven electric vehicles. *Journal of the Franklin Institute*, 50:71–94, 2014.

[13] R. Wang, Y. Chen, D. Feng, X. Huang, and J. Wang. Development and performance characterization of an electric ground vehicle with independently actuated in-wheel motors. *Journal of Power Sources*, 196:3962–3971, 2011.

[14] A. Watts, A. Vallance, A. Whitehead, C. Hilton, and A. Fraser. The technology and economics of in-wheel motors. *SAE Int. J. Passeng. Cars - Electron. Electr. Syst.*, pages 37–57, 2010.

[15] F. Wu, X. H. Yang, A. Packard, and G. Becker. Induced l^2-norm control for LPV systems with bounded parameter variation rates. *International Journal of Nonlinear and Robust Control*, 6:983–998, 1996.

[16] F.-K. Wu, T.-J. Yeh, and C.-F. Huang. Motor control and torque coordination of an electric vehicle actuated by two in-wheel motors. *Mechatronics*, 23:46–60, 2013.

[17] L. Xiong, Z. Yu, Y. Wang, C. Yang, and Y. Meng. Vehicle dynamics control of four in-wheel motor drive electric vehicle using gain scheduling based on tyre cornering stiffness estimation. *Vehicle System Dynamics*, 50:831–846, 2012.